

AIAA'84

AIAA-84-2370

**Noise Control Characteristics of
Synchrophasing — An Experimental
Investigation**

J. D. Jones and C. R. Fuller,
Virginia Polytechnic Institute and
State Univ., Blacksburg, VA

AIAA/NASA 9th Aeroacoustics Conference

October 15-17, 1984/Williamsburg, Virginia

NOISE CONTROL CHARACTERISTICS OF SYNCHROPHASING -- AN
EXPERIMENTAL INVESTIGATION

James D. Jones* and C. R. Fuller**
Virginia Polytechnic Institute and State University
Blacksburg, Virginia 24061

Abstract

A simplified cylindrical model of an aircraft fuselage is used to investigate the mechanisms of interior noise suppression of the synchrophasing technique. This investigation allows isolation of important parameters to define the characteristics of synchrophasing. The optimum synchrophase angle for maximum noise reduction is found for several interior microphone positions with pure tone source conditions. Noise reductions of up to 30dB are shown for some microphone positions, however, overall reductions are less. A computer algorithm is developed to decompose the modal composition of the cylinder vibration over a wide range of synchrophase angles. The circumferential modal response of the shell vibration is shown to govern the transmission of sound into the cylinder rather than localized transmission.

Nomenclature

| | |
|------------------|---|
| A_n | = complex modal amplitude coefficients, Eq. (1) |
| a | = radius of test cylinder, 0.254 m |
| B_n | = complex modal amplitude coefficients, Eq. (1) |
| f | = frequency |
| j | = $\sqrt{-1}$ |
| m | = 0, 1, 2, ... ∞ |
| N_p | = number of measuring points |
| n | = circumferential mode number |
| p | = 1, 2, 3, ... N_p |
| r, θ, x | = cylindrical coordinates |
| t | = time |
| w | = radial displacement |
| $\Delta\theta_p$ | = $2\pi/N_p$ |
| ϵ | = constant, $\epsilon = 2$ for $n = 0$; $\epsilon = 1$ for $n > 0$ |
| ϕ | = synchrophase angle |
| ω | = circular frequency |

Introduction

Due to the potential of significant fuel savings, recent interest has arisen over the use of advanced turboprop (A.T.P.) engines in commercial aircraft. However, preliminary investigations have shown that the interior levels of the aircraft

cabin exceed acceptable levels when A.T.P.'s are used. Several transmission paths for propeller noise¹ have been identified. The dominant path for propeller noise is the direct airborne path from the propeller blades through the cabin wall. Traditional passive techniques for noise control would require heavy damping material or additional mass around the propeller plane for the necessary noise reduction. The additional weight penalties for noise reduction would thus offset the potential fuel savings of A.T.P. engines, therefore, it is beneficial to investigate alternative methods for interior noise reduction. As discussed by Metzger¹, one of the most promising alternatives to passive techniques is synchrophasing. This technique involves synchronizing the relative rotational phase of the turboprop engines to achieve maximum interior noise reduction.

Promising results from previous experimental investigations^{2,3} have been acquired during in-flight testing in an actual aircraft fuselage. However, this procedure will not allow the investigator to isolate individual parameters and correspondingly study their effect on synchrophasing. To date, the physical mechanisms behind the synchrophasing concept are not fully understood. In addition, the in-flight testing can be expensive and time consuming. Therefore, a cost-effective simplified procedure is needed to perform preliminary investigations of the characteristics of synchrophasing as well as other interior noise effects.

In this investigation, an experimental procedure is developed to study the mechanisms of synchrophasing utilizing a simplified model of an aircraft fuselage in a controlled environment. The simplified model and sources used in this experimental investigation simulate propeller noise as transmitted into the aircraft cabin by the dominant airborne path, thereby, enabling a parametric study of synchrophasing to be performed. The information acquired is then used to define the characteristics of synchrophasing and to evaluate the potential propeller noise reduction. Hence, this experimental investigation leads to a better understanding of the synchrophasing concept and the mechanisms of sound transmission into aircraft cabins.

This experimental investigation is being done in conjunction with an analytical investigation⁴, the results of which are also being presented at the 9th AIAA Aeroacoustics Conference.

* Instructor, Mechanical Engineering
Student Member AIAA

** Visiting Professor, Mechanical Engineering

Experimental Setup and Procedure

A photograph of the experimental setup is presented in Fig. 1. The aircraft fuselage is modeled as a finite unstiffened aluminum cylinder 0.508 m in diameter by 1.245 m long. The cylinder was formed from a 1.63 mm thick aluminum sheet and has an epoxy-bonded butt-joint seam with a 5 mm wide exterior strap. Future investigations will involve studying the effects of more complex cylinder geometries, however, the purpose of this paper is to present preliminary results. The cylinder is sealed at both ends with 1.9 cm thick wooden end caps and is freely supported at the ends. The noise disturbances due to the propellers are modeled initially as monopole sources. Each monopole source is composed of a pair of 60-watt University Sound driver units. Extension tubes are attached to the driver units for the purpose of bringing the driver exits closer together thereby enabling the pair of drivers to more closely approximate a point source. By using two driver units instead of one, source levels can be increased enough to eliminate most signal-to-noise ratio problems. In addition, this will enable the pair of drivers to be used as a dipole source for future investigations. A monopole source is mounted on each side of the cylinder at the axial centerline to simulate the noise disturbances due to the propellers. The source height can be varied to study the effect of asymmetric loading on synchrophasing, however, for this investigation both source heights are fixed at the vertical centerline of the cylinder. The sources are rigidly mounted to the grated floor of the anechoic chamber such that end of the extension tubes are 10.8 cm from the cylinder. To simulate free-field conditions, the experiments are performed in a 2.3 x 2.6 x 4 m anechoic chamber which has a low frequency cutoff of 250 Hz.

A schematic diagram of the experimental setup showing model details and microphone locations is presented in Fig. 2. Three 6-mm-diameter B & K condenser microphones are mounted on an interior traversing mechanism at radial positions $r/a = 0.150, 0.513, \text{ and } 0.925$. The microphone cables are passed through a hole in one of the wooden end plates which is subsequently sealed with modeling clay. These three microphones are used to evaluate the axial, radial, and circumferential pressure

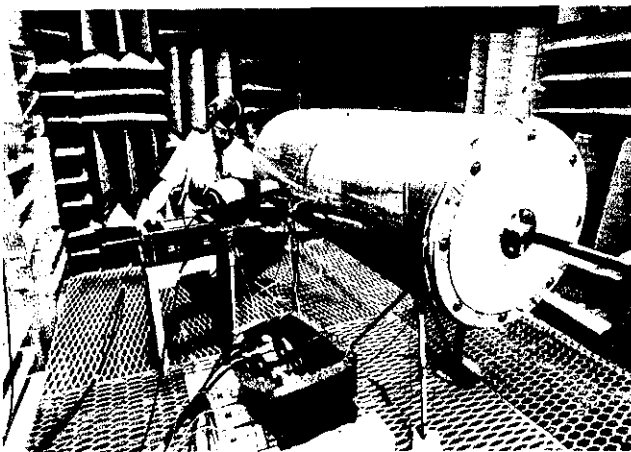


Fig. 1 Photograph of Experimental Setup.

distribution inside the cylinder. Another 6-mm-diameter B & K condenser microphone is used to measure the axial and circumferential pressure distribution on the exterior of the cylinder. In addition, two 6-mm-diameter condenser B & K microphones are positioned 5.4 mm directly in front of the two monopole sources and are used to set the amplitude and relative phase (i.e., synchrophase angle) of each source.

A schematic diagram of the data acquisition system is presented in Fig. 3(a). All microphone signals are conditioned with B & K signal conditioners and amplified and filtered of low frequency noise with Ithaco amplifiers before being fed into a switching box. Nine B & K accelerometers are mounted equally spaced around the circumference of the cylinder in the propeller plane ($x/a = 0.0$) to measure the modal response of the shell due to source excitation. The accelerometer signals are conditioned and are fed into the switching box. As it is necessary to locate both signal conditioners in the anechoic chamber, the exterior walls of the signal conditioner boxes are lined with a 12.7-mm-thick flexible polyurethane polyester foam to reduce acoustic scattering. All of the microphone and accelerometer signals are in turn processed with a two channel Zonic 5003 Fast Fourier Transformer (FFT). The cutoff frequency was set to 1500 Hz giving a frequency bandwidth of 7.3 Hz. A phase meter and oscilloscope are used to monitor the amplitudes, relative phase, and waveforms of the signals from the source microphones. The oscilloscope is also used to monitor the remaining microphone and accelerometer signals for distortions and clipping before data acquisition is initiated.

A schematic diagram of the source generation system is presented in Fig. 3(b). The reference pure tone signal for the noise source is generated by a Wavetek function generator and is monitored by an HP frequency counter. The reference signal is fed into a four channel gain-phase board where the gain and phase of the first two channels are set

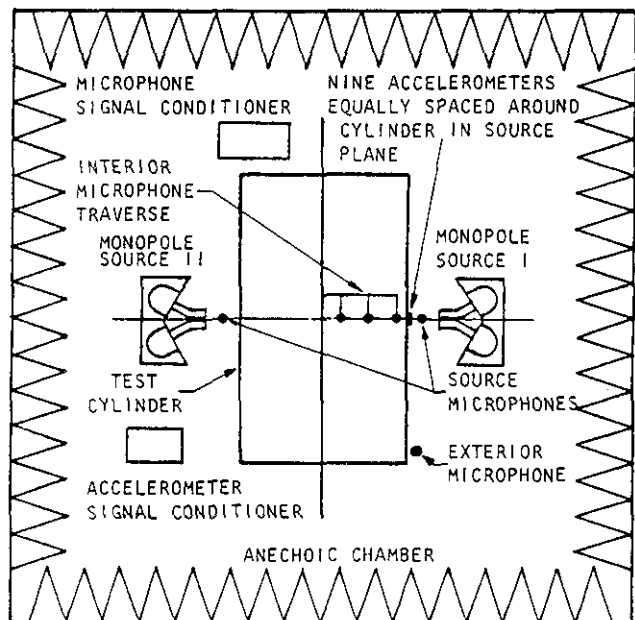


Fig. 2 Schematic Diagram of Experimental Setup.

based upon the signals from the source microphones. The signals from the gain-phase board are then amplified and sent to the monopole sources. A digital voltmeter is used to monitor the output voltages of the amplifiers to ensure that the sources are not being overloaded.

The interior microphones were initially positioned horizontally in the source plane towards source 1 (i.e., $x/a = 0.0$, $\theta = 0^\circ$) as shown in Fig. 2. Pressure measurements were recorded for the three radial microphone stations over the range of synchrophase angles of $\phi = 0$ to 360 using 45 degree phase increments. Additional pressure measurements were recorded at five degree increments around the optimum synchrophase angle of each interior microphone. While in the propeller plane, this procedure is repeated in the upper half of the cylinder at four additional circumferential positions, $\theta = 45, 90, 135,$ and 180 degrees. This procedure is also repeated in the horizontal source plane (at $\theta = 0^\circ$) at axial positions $x/a = 0.4, 0.8$ and 1.6 . Exterior microphone measurements were recorded at fifteen axial positions in the horizontal source plane (at $\theta = 0^\circ$) for synchrophase angles of $\phi = 0$ and 180 degrees. Finally, exterior microphone measurements were recorded in the propeller plane at seven circumferential positions for synchrophase angles of $\phi = 0$ and 180 degrees. All measurements were completed for pure tone source conditions of 680 and 708 Hz. These frequencies were chosen because they correspond to typical scaled fundamentals of the propeller noise. A third case was run with the source conditions again set to 708 Hz. However, for this case a layer of 12.7 -mm-thick flexible polyurethane polyester foam was placed on the interior of the cylinder covering 145 degrees of the bottom of the cylinder.

Modal Decomposition of Shell Vibration

The radial vibration response of the cylinder was measured for the modal decomposition algorithm. The relative amplitudes and phases of the nine equally spaced accelerometers were measured over a range of synchrophase angles from $\phi = 0$ to 360 degrees using 45 degree phase increments. Results from the decomposition algorithm defined the relative modal composition of the cylinder thereby enabling the dominant mode of the cylinder to be determined for various synchrophase angles. The modal composition of the cylinder is an essential element in understanding how sound is transmitted into the model.

The decomposition technique used in this investigation is similar to methods proposed by Moore and Silcox and Lester⁶. The radial displacement of a cylinder at any given time can be represented by a Fourier series of sines and cosines as follows.

$$\tilde{w}(\theta, t) = \sum_{n=0}^{\infty} [A_n \cos(n\theta) + B_n \sin(n\theta)] e^{j\omega t} \quad (1)$$

When a cylinder is excited, circumferential waves propagate in both directions around the cylinder combining to create an interference pattern or standing wave. To solve for the complex modal amplitudes A_n and B_n , equation (1) is multiplied by $\cos(m\theta)$ and $\sin(m\theta)$, respectively, and integrated from 0 to 2π . Thus,

$$\int_0^{2\pi} \tilde{w}(\theta) \cos(m\theta) d\theta = \sum_{n=0}^{\infty} \left[\int_0^{2\pi} A_n \cos(n\theta) \cos(m\theta) d\theta \right] \quad (2)$$

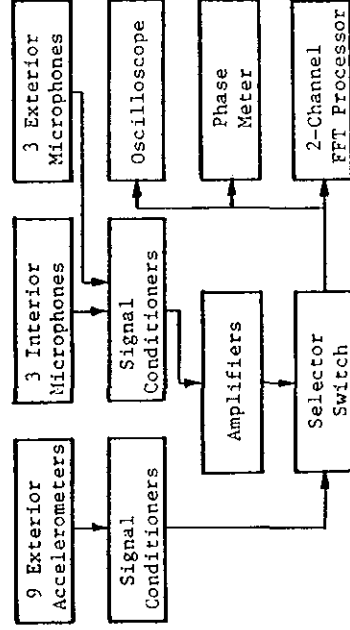
$$= \sum_{n=0}^{\infty} \left[\int_0^{2\pi} B_n \sin(n\theta) \cos(m\theta) d\theta \right] + \int_0^{2\pi} \tilde{w}(\theta) \sin(m\theta) d\theta$$

$$= \sum_{n=0}^{\infty} \left[\int_0^{2\pi} A_n \cos(n\theta) \sin(m\theta) d\theta \right] + \int_0^{2\pi} B_n \sin(n\theta) \sin(m\theta) d\theta \quad (3)$$

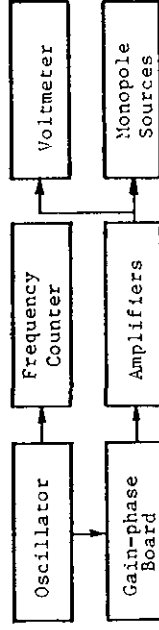
where $m = 0, 1, 2, 3, \dots, \infty$ and the time dependence $e^{j\omega t}$ has been omitted. By utilizing the orthogonality characteristics of the Fourier series, equations (2) and (3) can be reduced and rearranged to solve explicitly for the modal amplitudes. The resulting equations are

$$A_n = \frac{1}{\epsilon\pi} \int_0^{2\pi} \tilde{w}(\theta) \cos(n\theta) d\theta \quad (4)$$

$$B_n = \frac{1}{\epsilon\pi} \int_0^{2\pi} \tilde{w}(\theta) \sin(n\theta) d\theta \quad (5)$$



(a) Data Acquisition System



(b) Source Generation System

Fig. 3 Schematic Diagram of Instrumentation.

where $\epsilon = 2$ for $n = 0$

$\epsilon = 1$ for $n > 0$

$n = 0, 1, 2, 3, \dots, \infty$

If $w(\theta)$ is known completely as a function of θ , all of the modal amplitudes can be determined. In practice, however, $w(\theta)$ is known only at discrete points around the cylinder. Therefore, the integrals of equations (4) and (5) can be represented as Fourier summations of the form

$$A_n = \frac{1}{\epsilon\pi} \sum_{p=1}^{N_p} w(\theta_p) \cos(n\theta_p) \Delta\theta_p \quad (6)$$

$$B_n = \frac{1}{\epsilon\pi} \sum_{p=1}^{N_p} w(\theta_p) \sin(n\theta_p) \Delta\theta_p \quad (7)$$

where N_p is the number of circumferential positions where measurements are acquired and $\Delta\theta = 2\pi/N$ for equally spaced measuring points. In essence, the summation is an approximation to the integral but since the sine and cosine functions are periodic and the integration is done over one period, the error cancels out. However, this is true only if the number of the highest order mode generated is less than or equal to $N_p/2$ (Nyquist criteria). In addition, if one of the measuring points is positioned on a node the number of measuring points is reduced by one, as no information is acquired at this position.

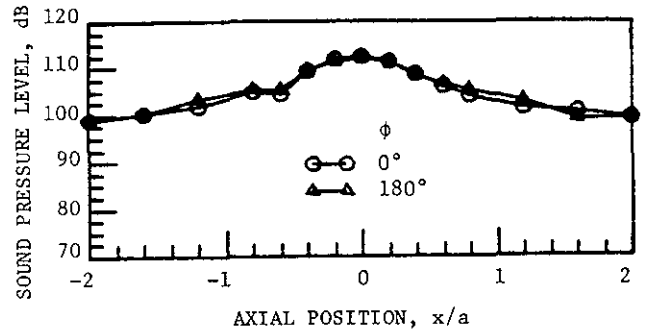
In practice, the assumed mode shapes are being fitted to the measured points, so that measurement errors or contributions from modes excluded from the decomposition may cause serious errors in the results of the decomposition. As long as the contributions from the dominant modes are included in the decomposition, the errors due to higher order modes are negligible. One method to check the decomposition results is to regenerate the radial displacements by substituting the modal amplitudes from the decomposition back into the Fourier series. A reproduction of the measured radial displacements gives credibility to the decomposition results.

In practice, the most effectively excited modes are the $n = 1$ and $n = 2$ modes. Therefore, the highest order mode decomposed for this investigation was limited to the $n = 4$ mode. Thus, nine equally spaced measuring points were used in this investigation. This ensures that there are at least enough measuring points off nodal positions to decompose five modes.

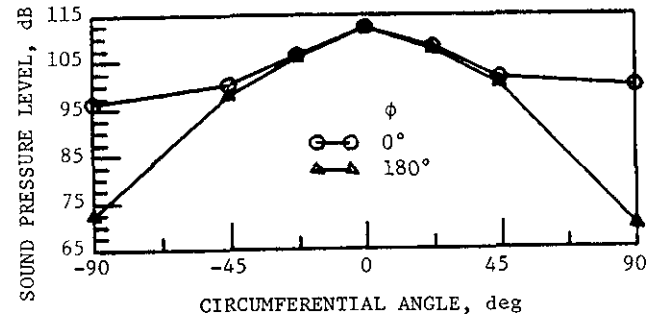
Results and Discussions

The results presented here are from the case with pure tone source conditions of 680 Hz. This case was chosen because it clearly defines the basic characteristics of synchrophasing.

Figures 4(a) and 4(b) show a comparison of the axial and circumferential pressure distributions on the exterior of the cylinder for synchrophasing angles of $\phi = 0$ and 180 degrees. Although propeller sources are better modeled as dipoles, the



(a) Axial Pressure Distribution at $\theta = 0^\circ$



(b) Circumferential Pressure Distribution at $x/a = 0.0$

Fig. 4 Exterior Pressure Measurements on Cylinder for $f = 680$ Hz.

axial and circumferential pressure distributions on the exterior of the cylinder due to the monopole sources used in this investigation are surprisingly similar to those measured on the exterior of an actual twin-engine turboprop aircraft fuselage. The axial pressure distribution on the exterior of the cylinder is symmetric about the propeller plane and decays about 13 dB by two cylinder radii. The similarity between this result and those from reference 7 implies that the pressure forcing function at the fuselage surface is due to the near field of each source or a very directional source. The synchrophase angle appears to have negligible effect on the axial pressure distribution at $\theta = 0$ degrees. However, the synchrophase angle has a significant effect on the circumferential pressure distribution for $\theta > 45$ degrees. This indicates that the near field of the source has substantially decayed in this region thereby allowing diffraction effects around the cylinder to become important. The circumferential pressure distribution is symmetric about the horizontal source plane and decays 13-16 dB for a synchrophase angle of $\phi = 0$ degrees and 40-42 dB for a synchrophase angle of $\phi = 180$ degrees. The more rapid decay in the circumferential pressure distribution for a synchrophase angle of $\phi = 180$ degrees can be explained using an interference interpretation. Near a point of symmetry between the sources (i.e., $\theta = 90^\circ$), cancellation occurs as the contribution from each source is relatively equal. However, in a region near $\theta = 0$ or 180 degrees the contribution from each individual source dominates the exterior pressure field and the synchrophase angle has little effect.

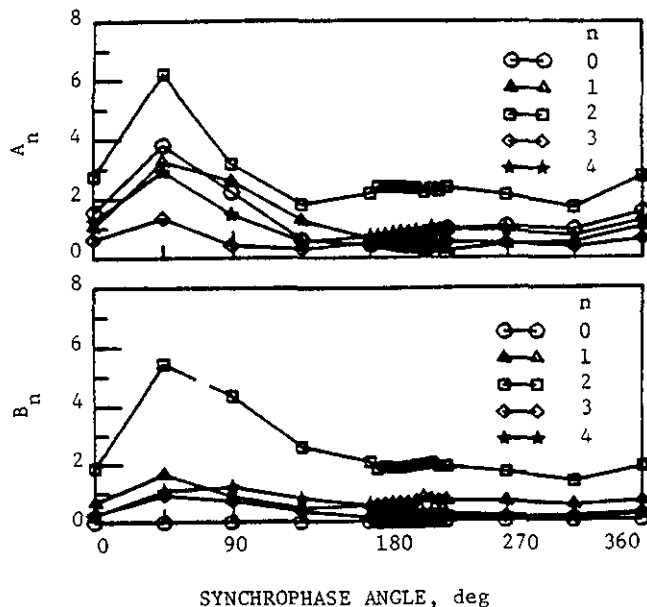


Fig. 5 Relative Modal Amplitudes of the Cylinder at $x/a = 0.0$ and $f = 680$ Hz.

Figure 5 shows the relative circumferential modal amplitudes of the cylinder versus synchrophase angle in the propeller plane for modes $n = 0$ to 4. The modal response of the cylinder is dominated by the $n = 2$ circumferential mode. For an ideal cylinder with the sources symmetrically positioned as shown in Fig. 2, the B_n modes should theoretically be zero. However, the decomposition results show significant B_n modes with the $n = 2$ mode dominating. The presence of significant B_n modes are most likely caused by cylinder asymmetry or the presence of the butt-joint seam along the cylinder leading to coupling effect with the A_n modes. The cylinder imperfections significantly alter the modal composition of the cylinder and the contained acoustic field, and therefore will effect the results of this experimental investigation. These results illustrate the need for a monitoring of the cylinder vibration to be carried out in conjunction with interior pressure measurements in order to successfully explain the resultant effects.

All of the modal amplitudes peak for a synchrophase angle of $\phi = 45$ degrees and generally decrease to a minimum near a synchrophase angle of $\phi = 180$ degrees. The results of the decomposition were checked by back substituting the modal amplitudes into the Fourier Series. Results showed that there was less than a 0.1% difference between the amplitudes and phases of the measured and reproduced radial displacements thereby giving credibility to the decomposition results.

Figure 6 shows the interior pressure measurements versus synchrophase angle measured in the propeller plane at the three radial microphone stations for circumferential position $\theta = 0$ degrees. The potential noise reduction varies from 15-25 dB depending on radial position. The optimum synchrophase angles for the three radial stations are all near $\phi = 180$ degrees. However, there is a slight variation in the optimum synchrophase angle

with radial position. The results from Fig. 6 can be explained by considering the radial vibration response of the shell. The monopole sources excite a series of circumferential modes in the shell which in turn couples to the contained acoustic field to govern the interior pressure distribution. Therefore, the total acoustic pressure at a given interior position is a superposition of acoustic pressures due to each circumferential mode generated in the cylinder. Theoretically, the optimum synchrophase angle to reduce the contributions from the even A_n modes and the odd B_n modes is $\phi = 180$ degrees. Similarly, the optimum synchrophase angle to reduce the contributions from the odd A_n modes and even B_n modes is $\phi = 0$ degrees. The dominant mode generated in the 680 Hz case is the $n = 2$ mode with significant contributions coming from the $n = 0, 1$ and 3 modes. At circumferential position $\theta = 0$ degrees, the contributions to the interior pressure levels from the B_n modes are theoretically zero. With the dominant A_n mode being even (i.e., $n = 2$), this implies that the optimum synchrophase angle should be near $\phi = 180^\circ$ as shown in Fig. 6. The small deviations from the expected optimum synchrophase angle of $\phi = 180$ degrees are due to the odd A_n modes generated which contributes somewhat to interior pressure distributions. In addition, asymmetry in the shell will cause some minor contributions from the B_n modes due to corresponding asymmetry of the contained acoustic field. The variation of the optimum synchrophase angle with radial position is due to differing contributions from the circumferential modes at the different radial positions. The interior pressure levels at $\theta = 0$ degrees are very sensitive to the synchrophase angle. This is true even near the cylinder wall at $r/a = 0.925$. However, as shown in Fig. 4(a) the exterior pressure distribution at $\theta = 0$ degrees is essentially unaffected by the synchrophase angle. This result indicates that sound is not being transmitted directly into the cylinder via a localized area of the wall but instead excites a series of circumferential modes which subsequently couple to the interior acoustic field. Thus, the representation of an aircraft fuselage as a finite flat plate or curved panel may be inadequate at low frequencies.

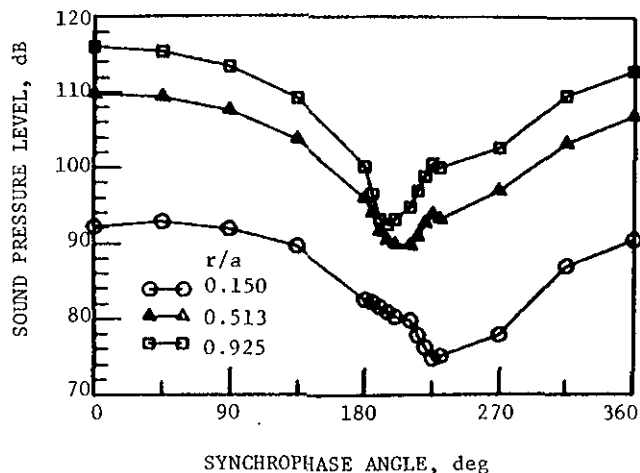


Fig. 6 Interior Pressure Measurements at $x/a = 0.0$, $\theta = 0^\circ$ and $f = 680$ Hz.

Figure 7 shows the interior pressure measurements versus synchrophase angle measured in the propeller plane at the three radial microphone stations for circumferential position $\theta = 45$ degrees. The potential noise reduction is about 10 dB for radial stations $r/a = 0.513$ and 0.925 and is about 23 dB for $r/a = 0.150$. The optimum synchrophase angles for all three radial stations increase to near $\phi = 260$ degrees. At $\theta = 45$ degrees, contributions from all of the decomposed A_n and B_n modes will be present except for the A_2 and B_4 modes. This results in approximately equal contributions from modes with an optimum synchrophase angle of $\phi = 180$ degrees and $\phi = 0$ (or 360) degrees. Therefore, an optimum synchrophase angle of 260 degrees is not surprising. Due to a lack of dominance of modes with an optimum synchrophase angle of either $\phi = 0$ or 180 degrees, the potential noise reduction by the synchrophasing technique has decreased significantly for radial station $r/a = 0.513$ and 0.925 . The $n = 0$ mode is the only mode which theoretically contributes to the acoustic pressure at the centerline of the cylinder. Therefore, as the cylinder's centerline is approached, the $n = 0$ mode will begin to dominate and the decrease in the potential noise reduction is not observed for radial station $r/a = 0.150$.

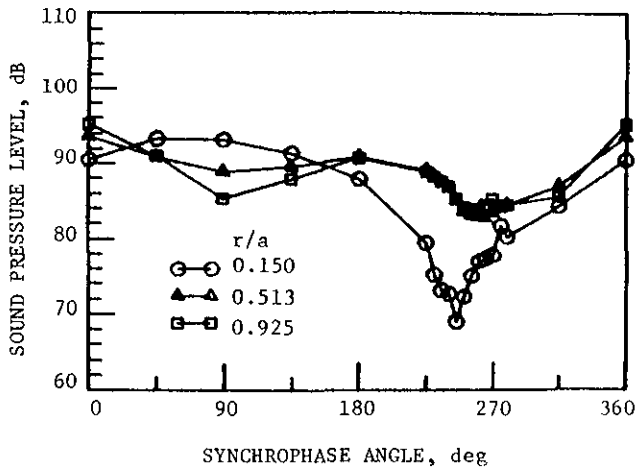


Fig. 7 Interior Pressure Measurements at $x/a = 0.0$, $\theta = 45^\circ$ and $f = 680$ Hz.

Figure 8 shows the interior pressure measurements versus synchrophase angle measured in the propeller plane at the three radial microphone stations for circumferential position $\theta = 90$ degrees. The potential noise reduction varies between 12-34 dB depending on radial position. The optimum synchrophase angle is $\phi = 180$ degrees for radial station $r/a = 0.513$ and 0.925 and $\phi = 0$ degrees for $r/a = 0.150$. All of the modes which have an optimum synchrophase angle of $\phi = 0$ degrees theoretically do not contribute to the interior acoustic field at $\theta = 90$ degrees. Therefore, large potential noise reductions are expected with optimum synchrophase angles of $\phi = 180$ degrees. Hence, the results at radial station $r/a = 0.150$ are quite surprising and difficult to explain. Apparently, the contributions from both A_n and B_n modes as well as imperfections in the cylinder combine to cause this unexpected result at $r/a = 0.150$.

As shown in Figs. 6, 7 and 8 the interior pressures levels in the propeller plane are generally greatest near the shell wall and decrease rapidly as the centerline of the cylinder is approached. The low pressure levels near the centerline of the cylinder ($r/a = 0.150$) are a result of the fact that the contributions to the interior acoustic field from all the modes except the $n = 0$ mode theoretically go to zero as the centerline of the cylinder is approached. Therefore, the pressure measurements at $r/a = 0.150$ are expected to be significantly lower than the other radial positions. This result gives additional support to the theory that the modal composition of the cylinder governs the interior acoustic field.

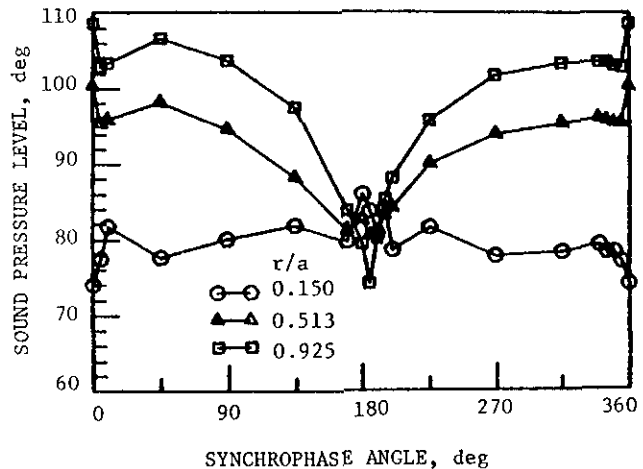


Fig. 8 Interior Pressure Measurements at $x/a = 0.0$, $\theta = 90^\circ$ and $f = 680$ Hz.

Figure 9 shows the interior pressure measurements versus synchrophase angle measured in the propeller plane at $r/a = 0.925$ for circumferential positions $\theta = 0, 45, 90, 135$ and 180 degrees. The interior pressure measurements versus synchrophase angle for $\theta > 90$ degrees vary as a mirror image of the results for $\theta < 90$ degrees except that the pressure levels for $\theta > 90$ degrees are about 8-13 dB lower than the pressure levels for $\theta < 90$ degrees. The nonsymmetric circumferential pressure distribution is caused by the presence of significant B_n modal amplitudes due to the imperfections in the shell. Similar results were found at radial stations $r/a = 0.150$ and 0.513 .

Figure 10 shows the interior pressure measurements versus synchrophase angle measured at $\theta = 0$ degrees for $r/a = 0.925$ and axial positions $x/a = 0.0, 0.4, 0.8$, and 1.6 . The interior pressure levels are very high in the propeller plane and decay rapidly with increasing axial position. This result is surprising for a finite cylinder and implies that the interior acoustic field is dominated by a near field in the propeller plane. The slight increase in the pressure levels at $x/a = 1.6$ are a result of a second peak in the axial standing wave. However, this standing wave peak is significantly lower than the dominant peak in the propeller plane. Thus, even for the finite unstiffened cylinder used in this experimental investigation the majority of the acoustic energy flows into the shell in a localized region near the propeller plane. This result tends to contradict

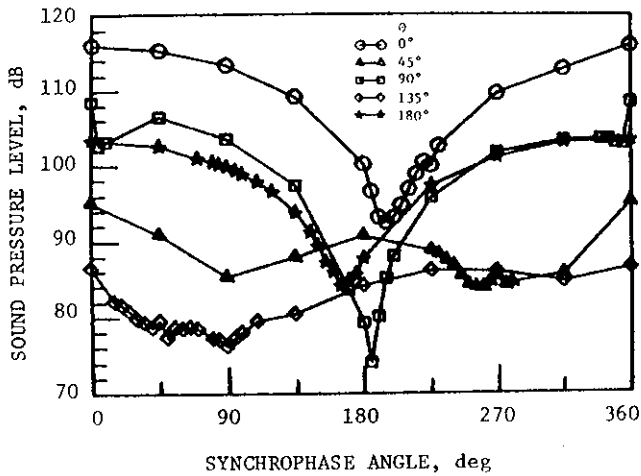


Fig. 9 Interior Pressure Measurements at $x/a = 0.0$, $r/a = 0.925$ and $f = 680$ Hz.

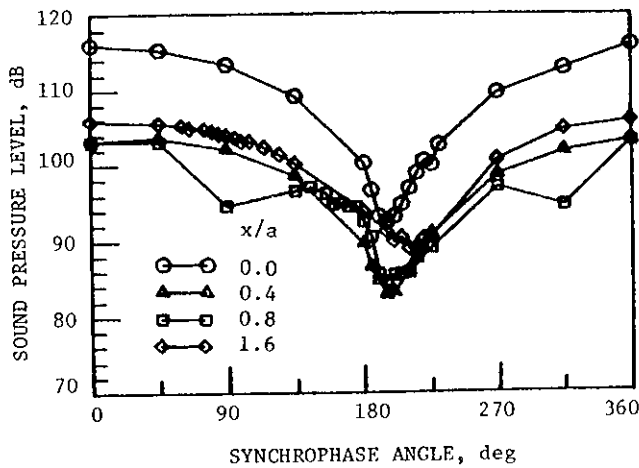


Fig. 10 Interior Pressure Measurements at $\theta = 0^\circ$, $r/a = 0.925$ and $f = 680$ Hz.

previous assumptions used in models for interior noise in aircraft and support the infinite shell model used in reference 4.

The results of Figs. 4(a) and 10 shows that the axial shell insertion loss varies dramatically with synchronphase angle. Thus, stabilization of the relative rotational phase of each propeller is essential before meaningful interior noise measurements can be obtained. The insertion loss presented by the shell wall is also better physically interpreted as a loss due to the modal response of the whole continuous cylinder surface rather than an attenuation due to a flat plate.

Although an infinite shell model with dipole sources is used in the analytical investigation of reference 4, the predicted synchronphasing characteristics are nearly identical to those obtained in this experimental investigation. The analytical exterior axial and circumferential pressure distributions are similar to those presented in Figs. 4(a) and 4(b) even though dipoles were used to model the propeller sources instead of monopoles. The optimum synchronphase angle and degree of attenuation from the analytical investigation closely

resemble the results presented here for the various interior microphone positions. Also, the analytical interior pressure distribution at $\theta = 0$ degrees was found to be very sensitive to the synchronphase angle while the exterior pressure distribution was unaffected by the synchronphase angle. Similar experimental results are shown in Figs. 4(a) and 10. The analytical interior acoustic field was dominated by a near field in the source plane implying that the majority of acoustic energy flows into the shell in a localized area near the propeller plane. Surprisingly, similar results were obtained from this experimental investigation even though a finite shell was used. This outcome implies that the end caps have a negligible effect on the interior acoustic field near the source plane. Thus, the results of this experimental investigation substantiate the assumptions of the infinite shell model used in reference 4.

Concluding Remarks

A simplified model of an aircraft fuselage was used to perform an experimental investigation of synchronphasing. The basic characteristics of synchronphasing have been defined. Potential noise reductions of 10-34 dB were measured throughout the interior of the cylinder. The optimum synchronphase angle and the degree of attenuation varies with location and depends on the modal composition of the cylinder and the relative contribution from each of these modes due to coupling with the interior acoustic field. The interior acoustic field was found to be dominated by pressure levels near the propeller plane thus implying that an infinite cylinder is a good model of an aircraft fuselage.

A computer algorithm was developed to decompose the modal composition of the cylinder for a range of synchronphase angles. The decomposition algorithm was found to be an essential tool for investigating the mechanisms of sound transmission into the cylinder. Modal decomposition results suggest that transmission of low frequency sound into aircraft cabins is governed by modal cylinder vibration rather than localized transmission. Also, the results indicate that the near-field or directional characteristics of propeller sources in a real aircraft strongly determine the nature of the transmission phenomena. Asymmetries in the cylinder were found to couple cylinder circumferential modes of vibration. Thus, any type of structural modifications (i.e., internal floors, ribs, etc.) will strongly affect the sound transmission.

The aircraft fuselage model and experimental procedure utilized in this investigation have been shown to be very successful in defining the characteristics of synchronphasing and other interior noise effects as well as giving insight into the mechanisms of sound transmission into aircraft cabins. The beginning of an experimental data base has been developed, however further studies are needed to completely understand the synchronphasing concept as well as other interior noise effects. Possible future investigations including studying the effects of multiple pure tones, the presence of an internal floor, asymmetric source loading, ribs, stiffeners, vibrational inputs at the wing attachments, internal damping and utilizing dipole sources instead of monopole sources to investigate the directional influence of the sources. Finally,

by coupling the results of the experimental model with the simplified analytical model⁴, a complete understanding of synchrophasing can be achieved.

Acknowledgments

The authors are grateful to the National Aeronautics and Space Administration's Langley and Lewis Research Centers for their support of this research under Grant NAG-1-390.

References

1. Metzger, F. B., "Strategies for Aircraft Interior Noise Reduction in Existing and Future Propeller Aircraft," SAE Paper 810560, 1981.
2. Johnston, J. F., Donham, R. E., and Guinn, W. A., "Propeller Signatures and Their Use," AIAA Paper 80-1035, 1980.
3. Magliozzi, B., "Synchrophasing for Cabin Noise Reduction of Propeller-Driven Airplanes," AIAA Paper 83-0717, 1983.
4. Fuller, C. R., "Noise Control Characteristics of Synchrophasing -- An Analytical Investigation," AIAA Paper 84-2369, 1984.
5. Moore, C. J., "Measurement of Radial and Circumferential Modes in Annular and Circular Fan Ducts," Journal of Sound and Vibration, Vol. 62, No. 2, 1979, pp. 235-256.
6. Silcox, R. J. and Lester, H. C., "Sound Propagation Through a Variable Area Duct: Experiment and Theory," AIAA Journal, Vol. 20, No. 10, 1982, pp. 1377-1384.
7. Mixson, J. S., Barton, C. K., Piersol, A. G., and Wilby, J. F., "Characteristics of Propeller Noise on an Aircraft Fuselage Related to Interior Noise Transmission," AIAA Paper 70-0646, 1979.